Research Square

Preprints are preliminary reports that have not undergone peer review.
They should not be considered conclusive, used to inform clinical practice,
or referenced by the media as validated information.

Celastrol Ameliorates Lupus by Promoting Apoptosis of Autoimmune T Cells and Preventing Autoimmune Response in MRL/lpr Mice

Tianhong Xie
Capital Medical University, Beijing Institute of Traditional Chinese Medicine
Huiqiang Liu
Beijing Hospital of Traditional Chinese Medicine, Capital Medical University
Xin Liu
Capital Medical University, Beijing Institute of Traditional Chinese Medicine
Xiang Liu
Capital Medical University, Beijing Institute of Traditional Chinese Medicine
Ping Li
liping@bjzhongyi.com

Capital Medical University, Beijing Institute of Traditional Chinese Medicine

Article

Keywords: Systemic lupus erythematosus, Autoimmunity, T cells, B cells

Posted Date: September 6th, 2023

DOI: https://doi.org/10.21203/rs.3.rs-3307451/v1

License: This work is licensed under a Creative Commons Attribution 4.0 International License.
Read Full License

Additional Declarations: No competing interests reported.

Version of Record: A version of this preprint was published at Lupus Science & Medicine on March 1st, 2024. See the published version at https://doi.org/10.1136/lupus-2023-001057.

Abstract

Celastrol is a bioactive constituent extracted from tripterygium wilfordii (Thunder God Vine). In the present study, we investigated whether Celastrol could have a regulatory effect on the autoimmune response in MRL/lpr mice. Our results demonstrated that Celastrol had a therapeutic effect on MRL/lpr mice by preventing the enlargement of the spleen and lymph nodes, alleviating renal injury, and reducing the levels of ANA and anti-dsDNA antibodies. Furthermore, Celastrol suppressed the *in vivo* inflammatory response in MRL/lpr mice by dramatically reducing the serum levels of multiple cytokines and production of antibody subsets. In addition, Celastrol treatment reduced in vitro anti-CD3 antibody stimulation-induced the number of Th1 and TNF-producing cells in CD4 + T cells of MRL/lpr mice. Celastrol treatment significantly affected B cell differentiation and prevented the generation of plasma cells from B cells in MRL/lpr mice by decreasing the number of activated and germinal center B cells. This contributed to the reduced secretion of autoantibodies in Celastrol-treated MRL/lpr mice. Celastrol treatment also affected T-cell differentiation and significantly reduced Tcm cell frequencies in MRL/lpr mice. Importantly, Celastrol treatment markedly and specifically promoted apoptosis of CD138 + T cells and suppressed autoimmune T-cell accumulation in MRL/lpr mice. The reduced number of CD138 + T cells further affected B-cell differentiation and subsequently resulted in the reduced number of autoreactive plasma cells which led to the reduced secretion of autoantibodies. Our results indicated that Celastrol had therapeutic effects on lupus by specifically promoting apoptosis of autoimmune T cells.

Introduction

Systemic lupus erythematosus (SLE) is a chronic inflammatory autoimmune disease that is involved in multisystem injuries. It predominantly affects females, especially between puberty and menopause [1,2], and is characterized by the production of autoantibodies [3,4], including anti-nuclear (ANA) and double-stranded DNA (dsDNA) antibodies. Epidemiological studies have demonstrated SLE to have a variable incidence rate and prevalence in different regions and environments worldwide [5–7]. Despite treatment advances in recent years, mortality in SLE patients remains high with significant geographic variations [1,8,9]. However, glucocorticoids are still used in clinical practice as a first-line treatment option and play an irreplaceable role in SLE treatment, despite the recent developments of therapeutic drugs such as belimumab and rituximab [10–15]. Glucocorticoids have shown significant therapeutic effects on SLE [10–13], however chronic usage of prednisone leads to irreversible damage or has substantial side effects in patients [13,16–18]. More treatment options with fewer side effects are required to substitute glucocorticoid treatment or reduce the dose of glucocorticoids, especially for patients who must be chronically administered glucocorticoids for SLE management.

Celastrol is a bioactive constituent extracted from tripterygium wilfordii (Thunder God Vine). Celastrol has been demonstrated to have a therapeutic effect on experimental disease models for chronic inflammatory and immune disorders [19–22], such as cancer and rheumatoid arthritis. Previous studies

also have demonstrated Celastrol could significantly alleviate lupus symptoms in SLE murine models [22–24]. However, the underlying mechanisms of the therapeutic effects of Celastrol on lupus in SLE murine models have not been deciphered. Neutrophil extracellular traps (NETs) have been shown to play a key role in innate immunity to pathogens [25]. In addition, NETs have been reported to be involved in self-antigen exposure such as self-DNA from dying cells in autoimmune diseases [25]. Recent studies have indicated that Celastrol could prevent *in vitro* NETs formation induced by inflammatory stimuli by downregulating the SYK-MEK-ERK-NF-κB signaling pathway [26]. In the present study, we further investigated in detail the underlying mechanisms of Celastrol for the treatment of SLE.

Autoantibodies initiate the autoimmune response and have a detrimental effect on multiple tissues and organs in SLE patients [27–29]. It is believed that B cells play a central role in adaptive immune responses, as they are specialized in producing antibodies. SLE is a disease that is highly variable and complex and both T and B cells participate in the progress of SLE [30–32]. Recent studies have shown that T cells play a more important role in the progression of lupus in SLE murine models [30,33,34]. In the present study, we investigated whether Celastrol could have a regulatory effect on the autoimmune response in Fas-deficiency MRL/lpr mice and the mechanism of Celastrol preventing autoimmune response.

Materials and methods

Mice

MRL/MPJ and MRL/lpr female mice were purchased from the Slac Laboratory (Shanghai, China). Mice were housed at 22 ± 1°C with a relative humidity of 50–60% and a 12-hour light/dark cycle.

Methods

4-week-old female MRL/MPJ and MRL/lpr mice were acclimatized for one week. MRL/MPJ mice were used as controls (ddH_2O, n = 9). MRL/lpr lupus mice were randomly grouped according to the different treatments as follows: vehicle (ddH_2O, n = 9), low dose of Celastrol (CL, n = 9) 2.5 mg/kg per day, high dose of Celastrol (CH, n = 9) 5.0 mg/kg per day, and prednisone (PNS, n = 6) 2.5 mg/kg per day. Celastrol (≥ 98%, HPLC, Batch no. DST200715-035, Fig. 1) was purchased from Desite Biotechnology Co., Ltd (Chengdu, China). Oral administration was performed daily from 9 to 18 weeks of age. On the 19th or 20th week, mice were anesthetized by 1% sodium pentobarbital (80 mg/kg) for serum collection and then euthanized by cervical dislocation with the following tissues harvested: lymph nodes and spleen (isolated and weighed), and kidneys (for histology).

Histology

To observe changes in renal pathology, paraformaldehyde-fixed kidneys were embedded in paraffin and then sectioned at 4-μm thickness. Hematoxylin and Eosin (H&E), periodic acid schiff (PAS), and Masson

trichrome staining were performed on the paraffin sections. Images of kidney tissues were obtained and analyzed using the Image-Pro Plus 6.0 (Media Cybernetics, Rockville, MD, USA)

Measurement of total IgG, anti-dsDNA IgG, and anti-nuclear antibodies in serum by ELISA

Total IgG, anti-dsDNA IgG, and anti-nuclear antibody (ANA) levels in the serum of mice were measured using an ELISA kit (total IgG ELISA kit, Thermo Fisher; anti-dsDNA IgG and ANA ELISA kit, Alpha Diagnostic International, San Antonio, TX, USA) according to the manufacturer's instructions. Optical density (OD) was determined at 450nm absorbance using a microplate reader.

Measurement of multiple cytokines and antibody isotypes in the serum using the Luminex platform

Serum levels of multiple cytokines and antibody subtypes were measured using the Luminex assay kits (Thermo Fisher, USA). Measurements were performed according to the manufacturer's instructions and analyzed on the Luminex™ platform.

Measurement of protein levels in the urine

Urine samples from individual mice were collected for 24 hours in the 16th week. Fresh urine samples were centrifuged at 300g for 10 min and then stored at -80°C. Protein levels in urine samples were determined using the Coomassie brilliant blue dye-binding assay kit and performed according to the manufacturer's instructions (Biokits Tech. Inc, Beijing, China).

Cellular stimulation

Anti-CD3 antibody (5μg/ml) or combined with 50 ng/ml phorbol 12-myristate 13-acetate (PMA), 1 μg/ml ionomycin and 2μM Monensin were used to stimulate and activate the cultured splenocytes from the mice.

Flow cytometry

Single-cell suspensions of splenocytes were obtained by filtering through a 70um cell strainer. Splenocytes were incubated on ice with CD16/CD32 monoclonal antibody (Thermo Fisher, eBiosience) for 15 minutes, and then red blood cells were lysed using lysis buffer (BD Bioscience). Splenocytes were then fixed and permeabilized (Fixation/Permeabilization solution, BD Bioscience) before intracellular staining. Cells were stained with the following antibodies for flow cytometry analysis: anti-CD3 PE-cy7, anti-CD3 APC-cy7, anti-CD4 FITC, anti-CD8 PerCP, anti-CD19 APC-cy7, anti-CD19 PE-cy7, anti-CD138 PE, anti-CD69 APC, anti-CD25 APC, anti-Foxp3 PE, anti-IL-4 APC, anti-IFN-γ PE-cy7, anti-TNF PE, anti-CD44 PE, anti-CD62L APC, Annexin V FITC, 7-AAD PerCP, anti-CD23, anti-B220 PerCP, anti-GL-7 APC, anti-MHC-II FITC, anti-CD23 APC, anti-CD21 PE, and anti-CD69 PE. Flow cytometry data were analyzed using Flowjo software version 10.6 for PC (Tree Star).

Statistical analysis

Data from all experiments were presented as mean ± standard deviation (SD) and analyzed using the SPSS software (SPSS, Inc., Chicago, IL, USA). Comparisons between the groups were performed for statistical significance using the Kruskal-Wallis H test followed by Dunn's post-test for analysis of non-parametric data and one-way analysis of variance followed by Tukey's post hoc test for analysis of parametric data. Mann-Whitney U test was used to assess statistical differences between two groups. Differences with P values less than 0.05 were considered statistically significant.

Results

Celastrol ameliorates lupus symptoms in MRL/lpr mice.

Compared to MRL/MPJ mice, significant enlargement of the spleen and lymph nodes, increased levels of ANA and anti-dsDNA IgG antibodies in the serum, obvious renal injuries, and elevated protein levels in the urine were observed in vehicle-treated MRL/lpr mice (Fig. 2). After administration of Celastrol (2.5mg/kg CL and 5.0mg/kg, CH), the increased weight of the spleen and lymph nodes, elevated levels of ANA and anti-dsDNA IgG antibodies in the serum, and elevated protein levels in the urine of MRL/lpr mice were significantly ameliorated (Fig. 2A, 2D, and 2E). Additionally, obvious renal injuries in vehicle-treated MRL/lpr mice, such as hyaline deposits, interstitial and perivascular cellular inflammatory infiltration, cellular crescent formation, glomerular fibrosis, glomerulosclerosis, and tubular cell necrosis were also significantly alleviated (Fig. 2B and 2C) in MRL/lpr mice after Celastrol treatment (2.5mg/kg CL and 5.0mg/kg, CH). These results demonstrated that Celastrol could have a significant therapeutic effect on lupus in MRL/lpr mice.

Celastrol reduces antibody secretion.

In vivo inflammation induced by immune complexes and activated complement results in multiple organ injuries to promote SLE development [35]. We observed multiple antibody subsets in the serum, i.e., total IgG, IgG1, IgG2a, IgG2b, IgG3, IgM, IgA, and IgE levels were increased in MRL/lpr lupus mice compared to MRL/MPJ mice (Fig. 3). After Celastrol administration (5.0mg/kg, CH), total IgG, IgG1, and IgG2b levels in the serum of MRL/lpr mice were significantly reduced compared to vehicle-treated MRL/lpr mice (Fig. 3A, 3B, and 3D).

Celastrol significantly affects B cell differentiation.

Compared to MRL/MPJ mice, B cells in splenocytes of vehicle-treated MRL/lpr mice were significantly reduced (Fig. 4A). Additionally, we observed the number of follicular B cells was significantly reduced (Fig. 4B), however, the number of marginal B cells was increased in vehicle-treated MRL/lpr mice compared to MRL/MPJ mice (Fig. 4B). Both MHC-II expression levels in B cells and activated B cells in vehicle-treated MRL/lpr mice were significantly increased compared to MRL/MPJ mice (Fig. 4C and 4D), however, no significant differences in the number of germinal center (GC) B cells between vehicle-treated

MRL/lpr mice and MRL/MPJ mice (Fig. 4E) were observed. Importantly, the number of plasma cells in splenocytes of MRL/lpr mice was much higher compared to MRL/MPJ mice (Fig. 4F).

Celastrol administration (5.0mg/kg, CH) significantly increased B cell frequency in splenocytes of MRL/lpr mice (Fig. 4A) and markedly reduced the number of activated B cells in total B cells of MRL/lpr mice (Fig. 4D). Furthermore, GC B cell frequency was significantly reduced in Celastrol-treated MRL/lpr mice (5.0mg/kg, CH) compared to vehicle-treated MRL/lpr mice (Fig. 4E). Plasma cell frequencies in CD3- cells of MRL/lpr mice after oral administration of Celastrol (2.5mg/kg CL and 5.0mg/kg, CH) were found to be dramatically reduced (Fig. 4F), however, Celastrol administration did not show significant effects on the frequencies of both follicular and marginal B cells in B cells of MRL/lpr mice (Fig. 4B). Celastrol treatment also failed to significantly reduce MHC-II expression in B cells of MRL/lpr mice (Fig. 4C).

Celastrol suppresses the inflammatory response.

Multiple cytokines levels, including IFN-γ, IL-6, IL-12, and TNF in the serum were significantly increased in MRL/lpr mice compared to MRL/MPJ mice (Fig. 5A). In addition, the T helper (Th) 1 cell frequency of CD4 + T cells in vehicle-treated MRL/lpr mice was significantly increased after 5h in vitro stimulation of splenocytes with anti-CD3 antibody compared to MRL/MPJ mice (Fig. 5B and 5C). However, the Th2 cell frequency of CD4 + T cells was reduced in vehicle-treated MRL/lpr mice compared to MRL/MPJ mice (Fig. 5B and 5C). Accordingly, the ratio of Th1/Th2 in vehicle-treated MRL/lpr mice was significantly increased compared to MRL/MPJ mice (Fig. 5B and 5C). Interestingly, the number of TNF-producing cells in CD4 + T cells of MRL/lpr mice was markedly reduced compared to MRL/MPJ mice after 5h in vitro stimulation of splenocytes with anti-CD3 antibody despite the higher TNF serum levels in vivo in MRL/lpr mice (Fig. 5D). Additionally, regulatory T (Treg) cell frequency in CD4 + T cells was reduced in vehicle-treated MRL/lpr mice (Fig. 5E).

In vivo inflammation of MRL/lpr mice was significantly reduced by Celastrol administration. After oral administration of 2.5mg/kg (CL) Celastrol, serum levels of TNF in MRL/lpr mice were significantly reduced compared to vehicle-treated MRL/lpr mice (Fig. 5A). IFN-γ and IL-6 levels in the serum of MRL/lpr mice treated with 5.0 mg/kg (CH) of Celastrol showed an even more striking decrease (Fig. 5A). Further, Th1 cell frequencies in CD4 + T cells of Celastrol-treated MRL/lpr mice (2.5mg/kg, CL and 5.0mg/kg, CH) were also significantly reduced after 5h in vitro stimulation of splenocytes with anti-CD3 antibody compared to vehicle-treated mice (Fig. 5B and 5C). Furthermore, Th2 cell frequency in CD4 + T cells (5.0mg/kg, CH) was also simultaneously reduced in splenocytes of Celastrol-treated MRL/lpr mice (Fig. 5B and 5C) after 5h in vitro anti-CD3 antibody stimulation. However, the ratio of Th1/Th2 after anti-CD3 antibody stimulation in vitro was not significantly affected by Celastrol administration (Fig. 5C). In addition, the frequency of TNF-producing cells in CD4 + T cells of Celastrol-treated MRL/lpr mice (2.5mg/kg CL and 5.0mg/kg, CH) was also strikingly reduced compared to vehicle-treated mice (Fig. 5D). However, the frequency of Treg cells in CD4 + T cells of MRL/lpr mice was not significantly affected by Celastrol administration (Fig. 5E).

Celastrol treatment reduces the frequency of Tcm in T cells.

Compared to MRL/MPJ mice, CD3 + T cell frequency was significantly increased in the splenocytes of vehicle-treated MRL/lpr mice (Fig. 6A). Furthermore, Double Negative (DN) T cells were also increased in CD3 + T cells of MRL/lpr mice (Fig. 6B). However, CD4 + and CD8 + T cell frequencies in splenocytes of vehicle-treated MRL/lpr mice were reduced compared to MRL/MPJ mice (Fig. 6B). Additionally, CD69 + cells, central memory (Tcm), and effector memory (Tem) T cell frequencies in CD3 + T cells of vehicle-treated MRL/lpr mice were significantly increased compared to MRL/MPJ mice (Fig. 6C, and 6D). However, CD44-CD62L- and native T (Tn) cell frequencies in CD3 + T cells of vehicle-treated MRL/lpr mice were reduced (Fig. 6D).

Oral administration of Celastrol did not significantly prevent the accumulation of T cells in MRL/lpr mice (Fig. 6A). However, DN T cell accumulation in CD3 + T cells of MRL/lpr mice after Celastrol treatment (2.5mg/kg CL and 5.0mg/kg, CH) was significantly alleviated compared to vehicle-treated MRL/lpr mice (Fig. 6B). In addition, CD4 + T cell frequency in splenocytes showed an obvious increase in MRL/lpr mice after Celastrol treatment (5.0mg/kg, CH) compared to vehicle-treated MRL/lpr mice (Fig. 6B). Celastrol treatment however did not show a significant effect on the frequency of activated T cells in MRL/lpr mice (Fig. 6C). Tcm cell frequencies in MRL/lpr mice after Celastrol treatment (2.5mg/kg CL and 5.0mg/kg, CH) were significantly reduced compared to vehicle-treated MRL/lpr mice, but Tem, Tn, and CD44-CD62L- T cell frequencies in CD3 + T cells of MRL/lpr mice were not significantly affected by Celastrol treatment (Fig. 6D).

Celastrol specifically promotes apoptosis of CD138 + T cells.

Fas deficiency and subsequent reduced apoptosis in CD138 + T cells result in CD138 + T cell accumulation in MRL/lpr mice [34]. We observed CD138 + T cell accumulation in CD3 + T cells of vehicle-treated MRL/lpr mice but not in MRL/MPJ mice (Fig. 7A). CD138 + cell frequencies were also significantly increased in CD4 + and DN T cells of vehicle-treated MRL/lpr mice compared to MRL/MPJ mice (Fig. 7B and 7C). However, CD138 + cell frequencies in CD3 + T cells and T cells subsets (DN and CD4 + T cells) were significantly reduced in MRL/lpr mice after treatment of Celastrol (2.5mg/kg CL and 5.0mg/kg, CH) compared to vehicle-treated MRL/lpr mice (Fig. 7A, 7B, and 7C). In addition, we observed the frequency of apoptotic cells was increased but the frequency of live cells was reduced in CD138 + T cells of Celastrol-treated (5.0mg/kg, CH) MRL/lpr mice compared to vehicle-treated MRL/lpr mice (Fig. 7D). However, the frequency of apoptotic cells was not increased and the frequency of live cells was also not reduced in CD138- T cells of Celastrol-treated (5.0mg/kg, CH) MRL/lpr mice compared to vehicle-treated MRL/lpr mice (Fig. 7E). Celastrol treatment also did not show significant effects on CD69 + cell frequencies in CD138 + T cells of MRL/lpr mice compared to vehicle-treated MRL/lpr mice (Fig. 7F).

Discussion

In the present study, Celastrol administration had a therapeutic effect on MRL/lpr mice by significantly preventing the enlargement of the spleen and lymph nodes, in addition to alleviating renal injuries, and reducing the production of ANA and anti-dsDNA antibodies. Celastrol treatment also showed significant effects on suppressing *in vivo* inflammation in MRL/lpr mice by reducing serum levels of multiple cytokines and antibody subsets in MRL/lpr mice. Celastrol treatment also reduced Th1 and TNF-producing cell frequencies in CD4 + T cells of MRL/lpr mice to suppress *in vivo* inflammation. Celastrol inhibited the accumulation of DN and CD138 + T cells in MRL/lpr mice and significantly decreased Tcm frequency in CD3 + T cells of MRL/lpr mice. Importantly, celastrol specifically promoted CD138 + T cells spoptosis by increasing apoptosis levels of CD138 + T cells but not CD138- T cells in MRL/lpr mice. The reduced accumulation of CD138 + T cells in MRL/lpr mice induced by Celastrol treatment resulted in a reduction of autoreactive plasma cells which subsequently contributed to the reduced secretion of autoantibodies. In addition, Celastrol prevented plasma cell formation from B cells in MRL/lpr mice by reducing the frequency of activated and germinal B cells in the B cell population, which further contributed to the reduced secretion of autoantibodies in Celastrol-treated MRL/lpr mice.

Syndecan-1/CD138 is a marker of plasma cells in lymphocytes that are believed to originate from B cells [36,37]. CD138 + T cells, which express both CD3 and CD138, have been reported recently to be plasmablastic B-cell neoplasms as observed in clinical cases [38]. However, these abnormal CD138 + cells have also been observed in murine systemic lupus erythematosus (SLE) models [34,39,40]. Previous studies have demonstrated CD138 + T cells in MRL/lpr mice to significantly promote autoantibody production both *in vivo* and *in vitro* indicating CD138 + T cells are comprised of autoreactive T cells in MRL/lpr mice [34]. Moreover, CD138 expression in CD3 + T cells plays a key role in the progression of lupus in MRL/lpr mice. In the present study, we observed DN T cell accumulation in MRL/lpr mice. DN T cell accumulation has been demonstrated to play an important role in promoting the progression of lupus in MRL/lpr mice [30]. Our results showed that Celastrol administration significantly prevented the accumulation of DN T cells in MRL/lpr mice. CD138 expression in CD3 + T cells significantly prevents the apoptosis of CD3 + T cells and significantly contributes to the accumulation of DN T cells in MRL/lpr mice (unpublished data in preview by Xie TH et al.). Importantly, CD138 expression in DN T cells also significantly increased FasL expression in DN T cells. However, DN T cells in MRL/lpr mice are strongly cytotoxic and overexpresses FasL, which results in autoimmune injuries of multiple tissues that express small amounts of Fas receptor [30,41]. CD138 expression in CD3 + T cells also significantly promotes the activation of CD3 + T cells in MRL/lpr mice (unpublished data in preview by Xie TH et al.). Recent studies also found that CD138 + T cells could strikingly contribute to the formation of plasma cells from B cells of MRL/lpr mice [33,34]. A previous study showed that the majority of CD138 + T cells were Tcm cells and were both CD44 + CD62 + cells [34]. Our study demonstrated that oral administration of Celastrol significantly reduced Tcm cell frequency in CD3 + T cells in MRL/lpr mice. Celastrol treatment simultaneously prevented CD138 + T cell accumulation by specifically promoting apoptosis of CD138 + T cells in MRL/lpr mice. We also observed reduced serum levels of ANA and anti-dsDNA antibodies in Celastrol-treated MRL/lpr mice. Our results demonstrated that reduced CD138 + T cell accumulation induced by Celastrol administration contributed to reduced *in vivo* autoantibody production in MRL/lpr mice. In addition, our results showed

that Celastrol could significantly reduce the frequency of CD138 + cells in DN T cells of MRL/lpr mice, which subsequently resulted in reduced frequency of DN T cells of splenocytes in MRL/lpr mice.

Immune complexes induce the release of multiple cytokines in the serum of MRL/lpr mice to subsequently promote and amplify *in vivo* inflammation in MRL/lpr mice [35,42]. In the present study, we observed that Celastrol significantly reduced the production of antibody subsets including total IgG, IgG1, and IgG2b, and reduced serum levels of multiple cytokines such as TNF, IFN-γ, and IL-6 to inhibit the progression of inflammation in MRL/lpr mice. Several studies have shown that T cell polarization in SLE manifests from Th1 to Th2 cells, and IFN-α promotes activated B cell differentiation into plasma cells, which plays an essential role in SLE disease progression [43,44]. However, our results showed that the frequency of Th1 cells but not Th2 cells in CD4 + T cells of MRL/lpr mice was significantly increased in addition to increased serum levels of IFN-γ. Moreover, the ratio of Th1/Th2 in MRL/lpr mice was simultaneously increased compared to MRL/MPJ mice. Numerous studies have demonstrated that IFN-γ plays an essential role in the development of lupus in MRL/lpr mice [42,45–47]. IFN-γ significantly promotes the proliferation and accumulation of DN T cells and significantly increases the expression of FasL on the surface of DN T cells in lupus mice [46,47]. Previous *in vivo* studies have also shown that the frequency of Th1 cells in fas-deficient lupus mice, but not Th2, was significantly increased [39,48]. Furthermore, studies have also suggested that IFN-γ and Th1 cells may be closely associated with lupus development and tissue injury in MRL/lpr mice [46,49,50]. Furthermore, IFN-γ is required for the TLR7-promoted development of autoreactive B cells [49]. Our results demonstrated that Celastrol could significantly prevent IFN-γ expression and reduce Th1 cell frequency in CD4 + T cells in MRL/lpr mice in addition to decreasing serum IFN-γ levels.

TNF-alpha, a pro-inflammatory cytokine, plays a contradictory role in SLE. Increased TNF levels in the serum, kidneys, and skin samples of SLE patients as well as in SLE murine models play an inflammatory role in SLE and promote organ injury [51,52]. However, TNF is also a cytokine that induces apoptosis in cytotoxic T cells by activating caspase-8 in target cells [53]. It has been reported [54,55] that anti-TNF therapies such as TNF antibodies and soluble TNF receptors are associated with the induction of autoantibodies. Several studies have also proposed that the contribution of TNF in SLE progression is limited, however, increased TNF levels have been shown to contribute to the elimination of DN T cells in SLE murine models resulting in the improvement of lupus symptoms [53]. We observed contradictory results showing that although serum levels of TNF in MRL/lpr mice were increased, interestingly, the frequency of TNF-producing cells in CD4 + T cells of MRL/lpr mice was significantly reduced compared to MRL/MPJ mice. Previous studies have reported that TNF blockade therapy alone could result in the induction of ANA and anti-dsDNA despite the frequency and clinical characteristics of anti-TNF-induced lupus (ATIL) varying between the different drugs [54]. In the present study, both Celastrol and prednisone significantly reduced serum TNF levels and TNF-producing cell frequencies in CD4 + T cells of MRL/lpr mice. However, Celastrol and prednisone administration did not result in ATIL symptoms in MRL/lpr mice.

B cells play a central role in the adaptive immune response. It is believed that autoreactive B cells in SLE can further differentiate into abnormal plasma cells that secrete autoantibodies after activation by self-antigen and autoreactive T cells [56–59]. Immature B cells originate from stem cells in the bone marrow and BCR diversity is generated by random rearrangement of gene segments during early B-cell development [60,61]. After positive selection, pre-B cells express mIgM and become immature B cells [60,62]. Autoreactive immature B cells will undergo apoptosis and be eliminated by negative selection [60,61]. However, the mechanism by which autoreactive B cells escape negative selection in SLE is still unclear. It is thought that Fas deficiency may result in the failure of apoptosis in autoreactive B cells in SLE murine models [63,64]. MHC-II with self-antigens expressed in activated autoreactive B cells interacts with autoreactive CD4 + T cells and activates autoreactive T cells [57,65]. In addition, activated autoreactive B cells differentiate into plasma cells secreting autoantibodies with the help of autoreactive CD4 + T cells [34,57,65]. Our results showed that Celastrol significantly reduced GC B cell frequencies in B cells of MRL/lpr mice and strikingly inhibited the activation of B cells in MRL/lpr mice. This in turn contributes to the reduced number of plasma cells to further prevent the formation of autoreactive plasma cells. In Celastrol-treated MRL/lpr mice, both reduced plasma cell numbers and reduced CD138 + T cell accumulation contribute to reducing the levels of autoantibodies produced.

Conclusion

We demonstrated that Celastrol had a therapeutic effect on lupus in MRL/lpr mice. It had a significant effect on reducing the serum levels of multiple cytokines and antibody subsets. Celastrol also reduced the frequency of Th1 and TNF-producing cells in CD4 + T cells of MRL/lpr mice to suppress inflammation which suppressing the development and amplification of autoimmune repsonse in lupus. Furthermore, Celastrol inhibited the accumulation of DN and CD138 + T cells in MRL/lpr mice by specifically increasing apoptosis levels of CD138 + T cells, to alleviate the enlargement of the spleen and lymph nodes. Reduced accumulation of CD138 + T cells in MRL/lpr mice induced by Celastrol also contributed to reducing the number of autoreactive plasma cells. This in turn reduced autoantibody secretion in MRL/lpr mice. In addition, Celastrol treatment also prevented plasma cell generation in MRL/lpr mice by reducing activated and germinal B cell frequency in B cells. Reduced generation of plasma cells from B cells in MRL/lpr mice treated with Celastrol further contributed to reducing autoantibody secretion.

Declarations

Authors' contribution

Tianhong Xie conceived the study and wrote the manuscript. Tianhong Xie and Ping Li designed the experiments. Tianhong Xie and Huiqiang Liu performed the laboratory work. Tianhong Xie and Xin Liu performed data analysis. Xiang Liu and Ping Li revised and edited the manuscript. All authors read and approved the final version of the manuscript for publication.

Conflicts of interest statement

All authors declare no conflict of interest.

Acknowledgments

We would like to acknowledge Dr. Sabry Hamza for editing this manuscript.

Funding

This work was funded by the Beijing Postdoctoral Research Foundation (ZZ2019-23) and the MiaoPu research foundation of the Beijing Institute of Traditional Chinese Medicine (MP-2020-45).

Data and material availability

The data generated in the present study may be requested from the corresponding author.

Ethics approval and study guideline

All animal experiments were approved by Institutional Animal Care and Use Committee (IACUC) of Institute of Basic Theory for Chinese Medicine, China Academy of Chinese Medicine Science (IACUC Issue No. IBTCMCACMS21-2105-07), and were carried out in accordance with Animal Research: Reporting of In Vivo Experiments (ARRIVE) guidelines and institutional regulations.

References

1. Kaul, A. *et al.* Systemic lupus erythematosus. *Nat Rev Dis Primers* **2**, 16039, doi:10.1038/nrdp.2016.39 (2016).
2. Dörner, T. & Furie, R. Novel paradigms in systemic lupus erythematosus. *Lancet* **393**, 2344-2358, doi:10.1016/S0140-6736(19)30546-X (2019).
3. Lisnevskaia, L., Murphy, G. & Isenberg, D. Systemic lupus erythematosus. *Lancet* **384**, 1878-1888, doi:10.1016/S0140-6736(14)60128-8 (2014).
4. Zharkova, O. *et al.* Pathways leading to an immunological disease: systemic lupus erythematosus. *Rheumatology* **56**, i55-i66, doi:10.1093/rheumatology/kew427 (2017).
5. Stojan, G. & Petri, M. Epidemiology of systemic lupus erythematosus: an update. *Curr Opin Rheumatol* **30**, 144-150, doi:10.1097/BOR.0000000000000480 (2018).
6. Parikh, S. V., Almaani, S., Brodsky, S. & Rovin, B. H. Update on Lupus Nephritis: Core Curriculum 2020. *Am J Kidney Dis* **76**, 265-281, doi:10.1053/j.ajkd.2019.10.017 (2020).
7. Gergianaki, I., Bortoluzzi, A. & Bertsias, G. Update on the epidemiology, risk factors, and disease outcomes of systemic lupus erythematosus. *Best Pract Res Clin Rheumatol* **32**, 188-205, doi:10.1016/j.berh.2018.09.004 (2018).
8. Durcan, L., O'Dwyer, T. & Petri, M. Management strategies and future directions for systemic lupus erythematosus in adults. *Lancet* **393**, 2332-2343, doi:10.1016/S0140-6736(19)30237-5 (2019).

9. Vukelic, M., Li, Y. & Kyttaris, V. C. Novel Treatments in Lupus. *Front Immunol* **9**, 2658, doi:10.3389/fimmu.2018.02658 (2018).
10. Wilhelmus, S. *et al.* Lupus nephritis management guidelines compared. *Nephrol Dial Transplant* **31**, 904-913, doi:10.1093/ndt/gfv102 (2016).
11. Pinheiro, S. V. B., Dias, R. F., Fabiano, R. C. G., Araujo, S. d. A. & Silva, A. C. S. E. Pediatric lupus nephritis. *J Bras Nefrol* **41**, 252-265, doi:10.1590/2175-8239-JBN-2018-0097 (2019).
12. Mok, C. C. *et al.* Overview of lupus nephritis management guidelines and perspective from Asia. *Int J Rheum Dis* **16**, 625-636, doi:10.1111/1756-185X.12212 (2013).
13. Dammacco, R. Systemic lupus erythematosus and ocular involvement: an overview. *Clin Exp Med* **18**, 135-149, doi:10.1007/s10238-017-0479-9 (2018).
14. Menon, M., Blair, P. A., Isenberg, D. A. & Mauri, C. A Regulatory Feedback between Plasmacytoid Dendritic Cells and Regulatory B Cells Is Aberrant in Systemic Lupus Erythematosus. *Immunity* **44**, 683-697, doi:10.1016/j.immuni.2016.02.012 (2016).
15. Sciascia, S. *et al.* Efficacy of belimumab on renal outcomes in patients with systemic lupus erythematosus: A systematic review. *Autoimmun Rev* **16**, 287-293, doi:10.1016/j.autrev.2017.01.010 (2017).
16. Golder, V. & Tsang-A-Sjoe, M. W. P. Treatment targets in SLE: remission and low disease activity state. *Rheumatology (Oxford)* **59**, v19-v28, doi:10.1093/rheumatology/keaa420 (2020).
17. Thong, B. & Olsen, N. J. Systemic lupus erythematosus diagnosis and management. *Rheumatology* **56**, i3-i13, doi:10.1093/rheumatology/kew401 (2017).
18. Gatto, M., Zen, M., Iaccarino, L. & Doria, A. New therapeutic strategies in systemic lupus erythematosus management. *Nat Rev Rheumatol* **15**, 30-48, doi:10.1038/s41584-018-0133-2 (2019).
19. Kannaiyan, R. *et al.* Celastrol inhibits tumor cell proliferation and promotes apoptosis through the activation of c-Jun N-terminal kinase and suppression of PI3 K/Akt signaling pathways. *Apoptosis* **16**, 1028-1041, doi:10.1007/s10495-011-0629-6 (2011).
20. Yan, C.-Y. *et al.* Celastrol ameliorates Propionibacterium acnes/LPS-induced liver damage and MSU-induced gouty arthritis via inhibiting K63 deubiquitination of NLRP3. *Phytomedicine* **80**, 153398, doi:10.1016/j.phymed.2020.153398 (2021).
21. An, L. *et al.* Inflammation-Targeted Celastrol Nanodrug Attenuates Collagen-Induced Arthritis through NF-κB and Notch1 Pathways. *Nano Lett* **20**, 7728-7736, doi:10.1021/acs.nanolett.0c03279 (2020).
22. Xu, X., Zhong, J., Wu, Z., Fang, Y. & Xu, C. Effects of tripterine on mRNA expression of TGF-beta1 and collagen IV expression in BW F1 mice. *Cell Biochem Funct* **25**, 501-507, doi:10.1002/cbf.1338 (2007).
23. Xu, X., Wu, Z., Xu, C., Ren, Y. & Ge, Y. Observation on serum anti-double stranded DNA antibodies of tripterine in systemic lupus erythematosus of (NZBxW)F1 mice. *Ann Rheum Dis* **62**, 377-378, doi:10.1136/ard.62.4.377 (2003).

24. Li, H. *et al.* Beneficial effect of tripterine on systemic lupus erythematosus induced by active chromatin in BALB/c mice. *Eur J Pharmacol* **512**, 231-237, doi:10.1016/j.ejphar.2005.02.030 (2005).
25. Döring, Y., Soehnlein, O. & Weber, C. Neutrophil Extracellular Traps in Atherosclerosis and Atherothrombosis. *Circ Res* **120**, 736-743, doi:10.1161/CIRCRESAHA.116.309692 (2017).
26. Yu, Y. *et al.* Celastrol inhibits inflammatory stimuli-induced neutrophil extracellular trap formation. *Curr Mol Med* **15**, 401-410, doi:10.2174/1566524015666150505160743 (2015).
27. You, M. *et al.* Ligation of CD180 inhibits IFN-α signaling in a Lyn-PI3K-BTK-dependent manner in B cells. *Cell Mol Immunol* **14**, 192-202, doi:10.1038/cmi.2015.61 (2017).
28. Dörner, T., Giesecke, C. & Lipsky, P. E. Mechanisms of B cell autoimmunity in SLE. *Arthritis Res Ther* **13**, 243, doi:10.1186/ar3433 (2011).
29. Kotzin, B. L. Systemic lupus erythematosus. *Cell* **85**, 303-306, doi:10.1016/s0092-8674(00)81108-3 (1996).
30. Alexander, J. J., Jacob, A., Chang, A., Quigg, R. J. & Jarvis, J. N. Double negative T cells, a potential biomarker for systemic lupus erythematosus. *Precis Clin Med* **3**, 34-43, doi:10.1093/pcmedi/pbaa001 (2020).
31. Chesnutt, M. S. *et al.* Enhanced lymphoproliferation and diminished autoimmunity in CD4-deficient MRL/lpr mice. *Clin Immunol Immunopathol* **87**, 23-32, doi:10.1006/clin.1997.4492 (1998).
32. Nagasu, A. *et al.* Sh3bp2 Gain-Of-Function Mutation Ameliorates Lupus Phenotypes in B6.MRL-Fas^{lpr} Mice. *Cells* **8**, 402, doi:10.3390/cells8050402 (2019).
33. Liu, L. & Akkoyunlu, M. Circulating CD138 enhances disease progression by augmenting autoreactive antibody production in a mouse model of systemic lupus erythematosus. *J Biol Chem* **297**, 101053, doi:10.1016/j.jbc.2021.101053 (2021).
34. Liu, L., Takeda, K. & Akkoyunlu, M. Disease stage-specific pathogenicity of CD138 (Syndecan 1)-expressing T cells in systemic lupus erythematosus. *Front Immunol* **11**, 1569, doi:10.3389/fimmu.2020.01569 (2020).
35. Sandhu, V. & Quan, M. SLE and Serum Complement: Causative, Concomitant or Coincidental? *Open Rheumatol J* **11**, 113-122, doi:10.2174/1874312901711010113 (2017).
36. Lu, L. D. *et al.* Depletion of autoreactive plasma cells and treatment of lupus nephritis in mice using CEP-33779, a novel, orally active, selective inhibitor of JAK2. *J Immunol* **187**, 3840-3853, doi:10.4049/jimmunol.1101228 (2011).
37. Calame, K. L. Plasma cells: finding new light at the end of B cell development. *Nat Immunol* **2**, 1103-1108, doi:10.1038/ni1201-1103 (2001).
38. Pan, Z. *et al.* CD3-positive plasmablastic B-cell neoplasms: a diagnostic pitfall. *Mod Pathol* **31**, 718-731, doi:10.1038/modpathol.2017.177 (2018).
39. Seagal, J., Leider, N., Wildbaum, G., Karin, N. & Melamed, D. Increased plasma cell frequency and accumulation of abnormal syndecan-1plus T-cells in Igmu-deficient/lpr mice. *Int Immunol* **15**, 1045-1052, doi:10.1093/intimm/dxg107 (2003).

40. Mohamood, A. S. *et al.* Fas-mediated apoptosis regulates the composition of peripheral αβ T Cell repertoire by constitutively purging out double negative T cells. *PLoS One* **3**, e3465, doi:10.1371/journal.pone.0003465 (2008).
41. Benihoud, K., Bonardelle, D., Bobé, P. & Kiger, N. MRL/lpr CD4- CD8- and CD8+ T cells, respectively, mediate Fas-dependent and perforin cytotoxic pathways. *Eur J Immunol* **27**, 415-420, doi:10.1002/eji.1830270211 (1997).
42. Tshilela, K. A. *et al.* Glomerular cytokine expression in murine lupus nephritis. *Clin Exp Nephrol* **20**, 23-29, doi:10.1007/s10157-015-1123-1 (2016).
43. Selvaraja, M. *et al.* Elevated interleukin-25 and its association to Th2 cytokines in systemic lupus erythematosus with lupus nephritis. *PLoS One* **14**, e0224707, doi:10.1371/journal.pone.0224707 (2019).
44. Ehrenfeld, M., Blank, M., Shoenfeld, Y. & Hidvegi, M. AVEMAR (a new benzoquinone-containing natural product) administration interferes with the Th2 response in experimental SLE and promotes amelioration of the disease. *Lupus* **10**, 622-627, doi:10.1191/096120301682430203 (2001).
45. Tan, W. *et al.* Let-7f-5p ameliorates inflammation by targeting NLRP3 in bone marrow-derived mesenchymal stem cells in patients with systemic lupus erythematosus. *Biomed Pharmacother* **118**, 109313, doi:10.1016/j.biopha.2019.109313 (2019).
46. Balomenos, D., Rumold, R. & Theofilopoulos, A. N. Interferon-gamma is required for lupus-like disease and lymphoaccumulation in MRL-lpr mice. *J Clin Invest* **101**, 364-371, doi:10.1172/JCI750 (1998).
47. Juvet, S. C. *et al.* Autocrine IFNgamma controls the regulatory function of lymphoproliferative double negative T cells. *PLoS One* **7**, e47732, doi:10.1371/journal.pone.0047732 (2012).
48. Tang, X. *et al.* Transplantation of dental tissue-derived mesenchymal stem cells ameliorates nephritis in lupus mice. *Ann Transl Med* **7**, 132, doi:10.21037/atm.2019.02.41 (2019).
49. Chodisetti, S. B. *et al.* Type II but Not Type I IFN Signaling Is Indispensable for TLR7-Promoted Development of Autoreactive B Cells and Systemic Autoimmunity. *J Immunol* **204**, 796-809, doi:10.4049/jimmunol.1901175 (2020).
50. Zhang, X. *et al.* Type I interferons protect neonates from acute inflammation through interleukin 10-producing B cells. *J Exp Med* **204**, 1107-1118, doi:10.1084/jem.20062013 (2007).
51. Aringer, M. & Smolen, J. S. Therapeutic blockade of TNF in patients with SLE-promising or crazy? *Autoimmun Rev* **11**, 321-325, doi:10.1016/j.autrev.2011.05.001 (2012).
52. Sabry, A. *et al.* Proinflammatory cytokines (TNF-alpha and IL-6) in Egyptian patients with SLE: its correlation with disease activity. *Cytokine* **35**, 148-153, doi:10.1016/j.cyto.2006.07.023 (2006).
53. Nagasu, A. *et al.* Sh3bp2 Gain-Of-Function Mutation Ameliorates Lupus Phenotypes in B6.MRL-Faslpr Mice. *Cells* **8**, 402, doi:10.3390/cells8050402 (2019).
54. Williams, E. L., Gadola, S. & Edwards, C. J. Anti-TNF-induced lupus. *Rheumatology* **48**, 716-720, doi:10.1093/rheumatology/kep080 (2009).

55. Katz, U. & Zandman-Goddard, G. Drug-induced lupus: an update. *Autoimmun Rev* **10**, 46-50, doi:10.1016/j.autrev.2010.07.005 (2010).
56. de la Varga-Martínez, R. *et al.* Autoreactive B-lymphocytes in SLE and RA patients: Isolation and characterisation using extractable nuclear and citrullinated antigens bound to immunobeads. *Eur J Immunol* **49**, 1107-1116, doi:10.1002/eji.201848065 (2019).
57. Laurent, L. *et al.* Prevention of lupus nephritis development in NZB/NZW mice by selective blockade of CD28. *Eur J Immunol* **47**, 1368-1376, doi:10.1002/eji.201746923 (2017).
58. Jackson, S. W. & Davidson, A. BAFF inhibition in SLE-Is tolerance restored? *Immunol Rev* **292**, 102-119, doi:10.1111/imr.12810 (2019).
59. Mihaylova, N. *et al.* Suppression of autoreactive T and B lymphocytes by anti-annexin A1 antibody in a humanized NSG murine model of systemic lupus erythematosus. *Clin Exp Immunol* **199**, 278-293, doi:10.1111/cei.13399 (2020).
60. Monroe, J. G. *et al.* Positive and negative selection during B lymphocyte development. *Immunol Res* **27**, 427-442, doi:10.1385/IR:27:2-3:427 (2003).
61. Xu, X. *et al.* An ontogenetic switch drives the positive and negative selection of B cells. *Proc Natl Acad Sci U S A* **117**, 3718-3727, doi:10.1073/pnas.1915247117 (2020).
62. Benhamou, D. *et al.* A c-Myc/miR17-92/Pten Axis Controls PI3K-Mediated Positive and Negative Selection in B Cell Development and Reconstitutes CD19 Deficiency. *Cell Rep* **16**, 419-431, doi:10.1016/j.celrep.2016.05.084 (2016).
63. Akagi, T., Yoshino, T. & Kondo, E. The Fas antigen and Fas-mediated apoptosis in B-cell differentiation. *Leuk Lymphoma* **28**, 483-489, doi:10.3109/10428199809058355 (1998).
64. Hancz, A., Koncz, G., Szili, D. & Sármay, G. TLR9-mediated signals rescue B-cells from Fas-induced apoptosis via inactivation of caspases. *Immunol Lett* **143**, 77-84, doi:10.1016/j.imlet.2012.02.006 (2012).
65. Chesnutt, M. S. *et al.* Enhanced lymphoproliferation and diminished autoimmunity in CD4-deficient MRL/ lpr mice. *Clin Immunol Immunopathol* **87**, 23-32., doi:10.1006/clin.1997.4492 (1998).

Figures

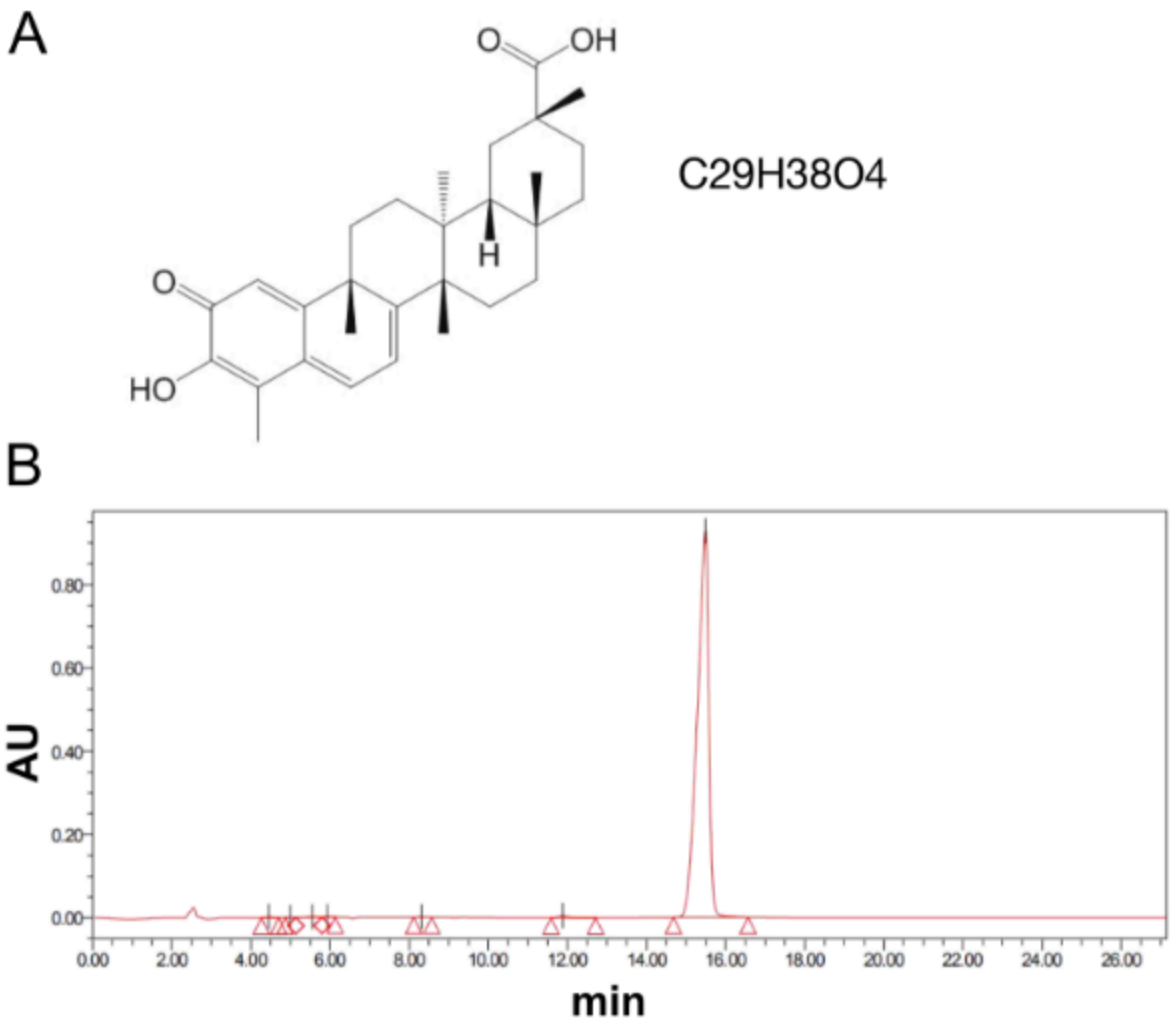


Figure 1

(A) Chemical structure of celastrol. (B) HPLC analysis of celastrol.

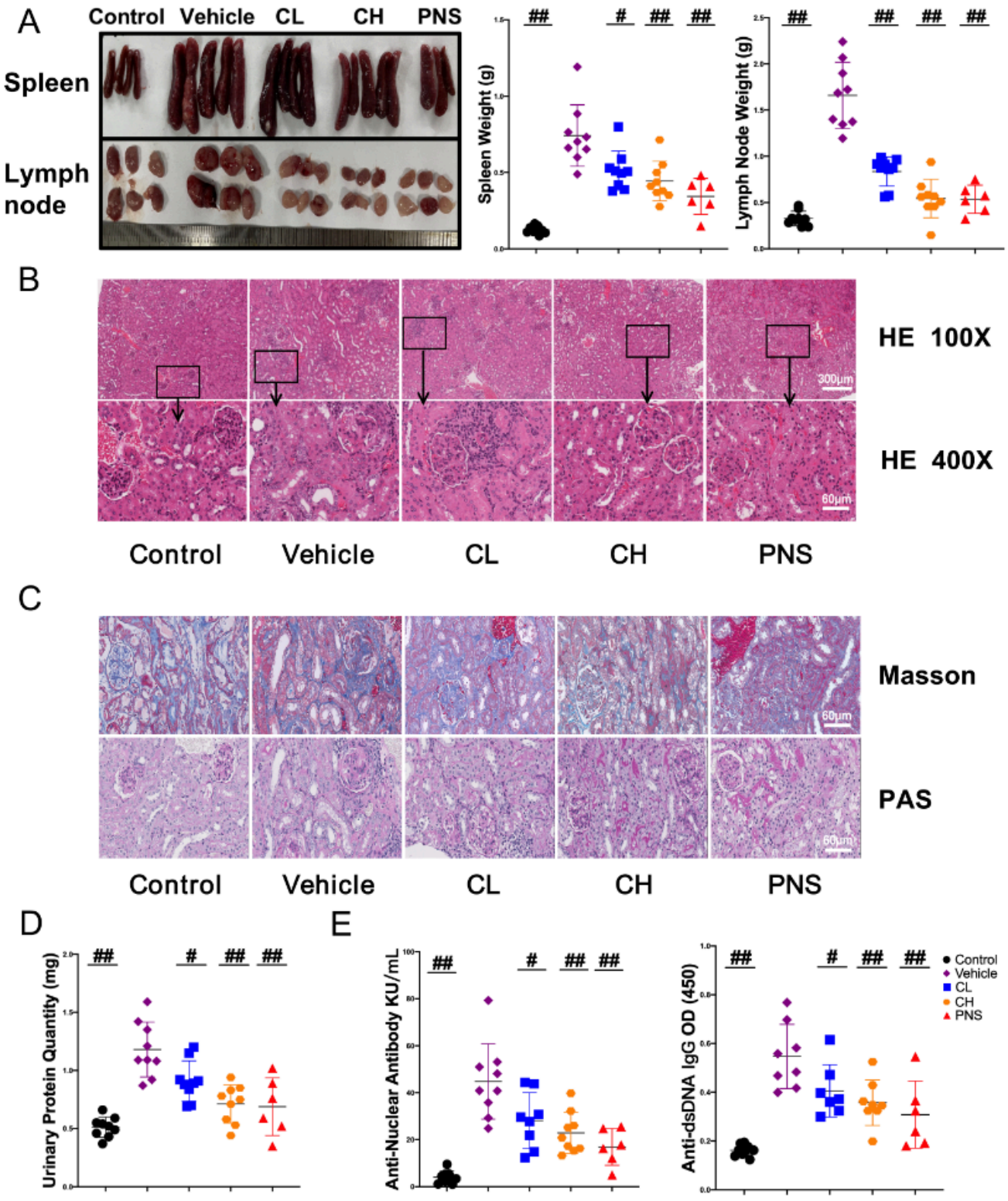


Figure 2

(A) Image of the spleen (top panels) and lymph nodes (bottom panels), with scatter plots showing the weight of the spleen and lymph nodes. (B) Renal tissue pathological sections were stained with HE, original magnification: 100× (top panels) and 400X (bottom panels), scale bar =300 μm and 60 μm. (C) Renal tissue pathological sections were stained with PAS and Masson, original magnification: 400X, scale bar =60 μm. (D) Scatter plots denote urinary protein quantity. (E) Scatter plots denote ANA and

anti-dsDNA antibody levels in the serum of mice. Data presented as mean±SD (n=6-9 mice per group) from 2-3 independent experiments: #P < 0.05, ##P < 0.01 by one-way analysis of variance.

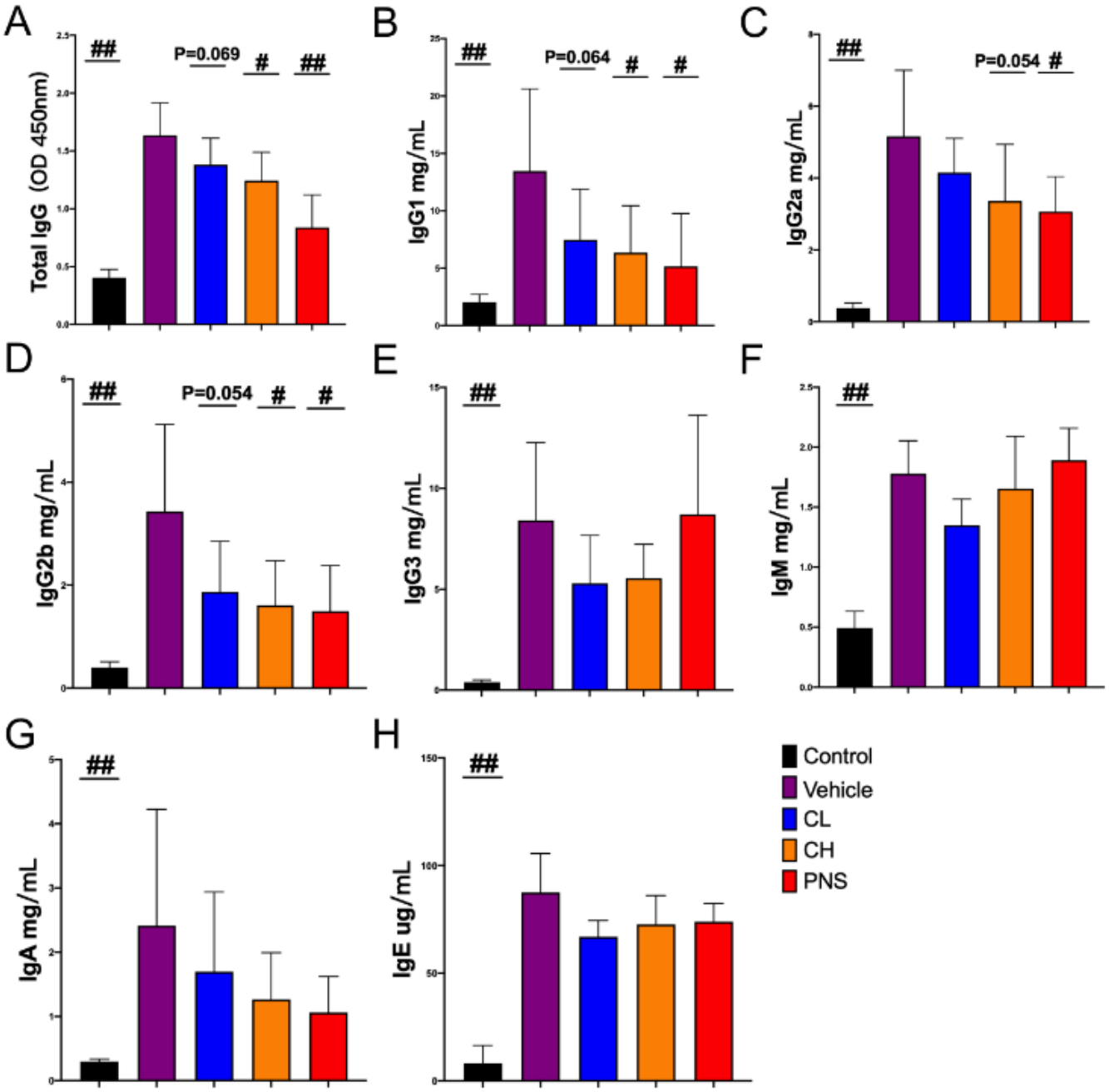


Figure 3

(A) Bars denote total IgG levels in the serum of mice. (B) Bars denote IgG1 levels in the serum of mice. (C) Bars denote IgG2a levels in the serum of mice. (D) Bars denote IgG2b levels in the serum of mice. (E) Bars denote IgG3 levels in the serum of mice. (F) Bars denote IgM levels in the serum of mice. (G) Bars denote IgA levels in the serum of mice. (H) Bars denote IgE levels in the serum of mice. Data presented as mean±SD (n=6-8 mice per group) from 2-3 independent experiments: #P < 0.05, ##P < 0.01 by Kruskal-Wallis H test (Figure 3D) or one-way analysis of variance.

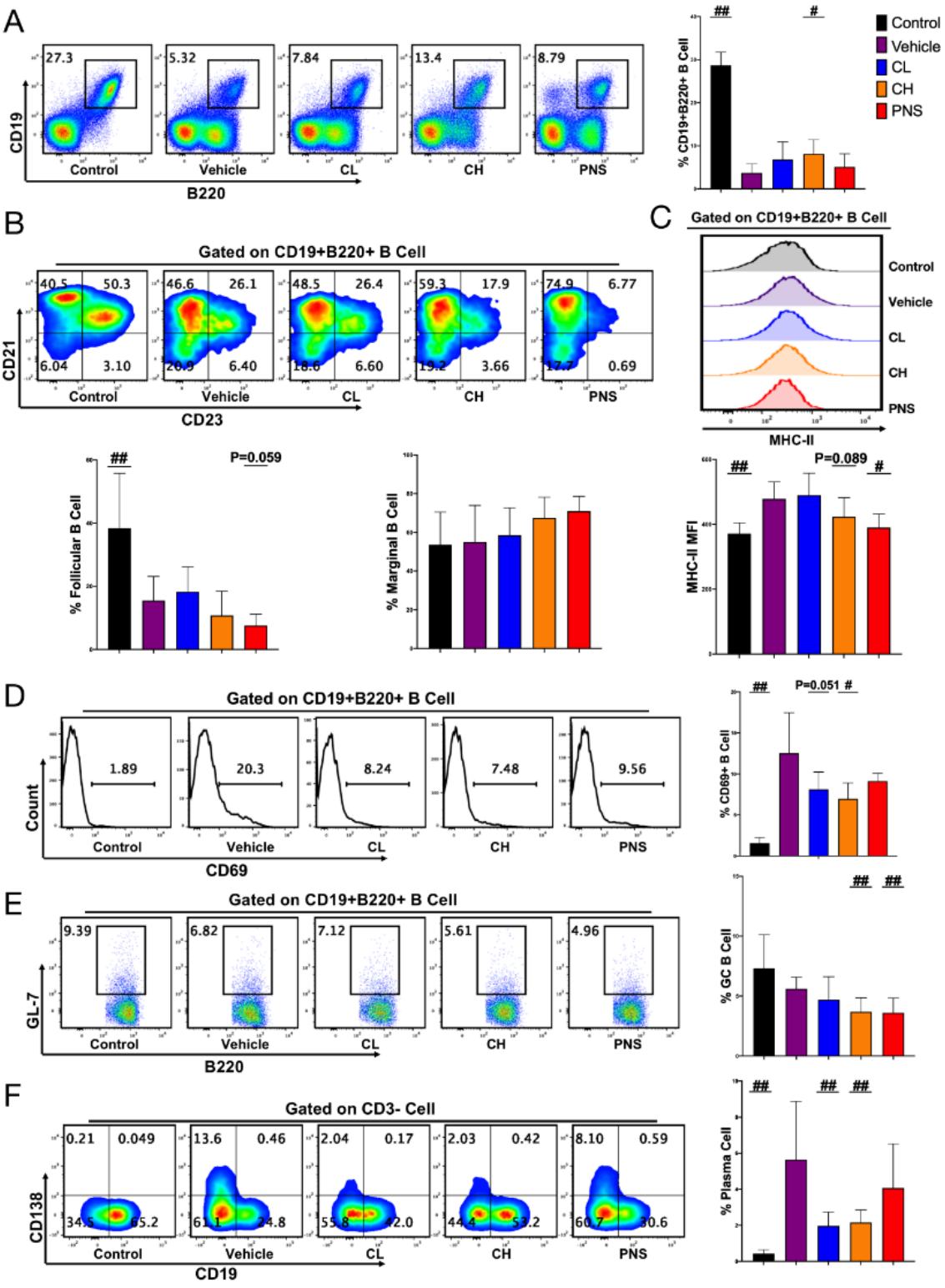


Figure 4

(A) Representative flow cytometry analyses and bars denoting the frequencies of CD19+B220+ B cells in the splenocytes of mice. (B) Representative flow cytometry analyses and bars denoting the frequencies of follicular (gated on CD19+B220+CD23+CD21int) and marginal zone (gated on CD19+B220+CD21+CD23-) B cells in B cells of mice. (C) Representative flow cytometry analyses and bars denoting MHC-II MFI for MHC-II expression levels in B cells (gated on CD19+B220+) of mice. (D)

Representative flow cytometry analyses and bars denoting the frequencies of CD69+ cells in B cells (gated on CD19+B220+) of mice. (E) Representative flow cytometry analyses and bars denoting the frequencies of germinal center B cells (gated on CD19+B220+GL-7+) in B cells of mice. (F) Representative flow cytometry analyses and bars denoting the frequencies of plasma cells (gated on CD138+CD19-) in CD3- cells of mice. Data presented as mean±SD (n=5-9 mice per group) from 2-3 independent experiments: #P < 0.05, ##P < 0.01 by Kruskal-Wallis H test(Figure 4F) or one-way analysis of variance.

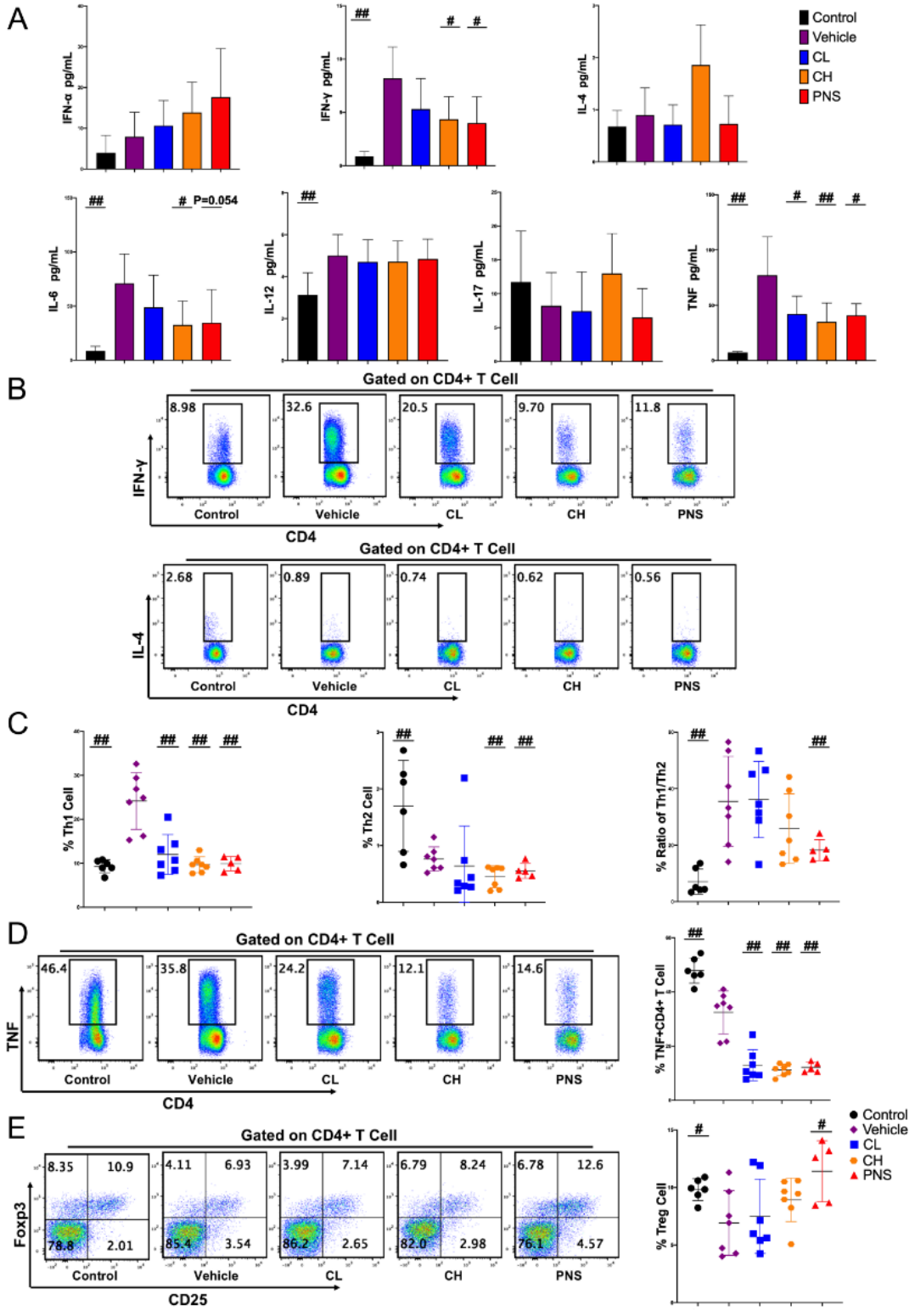


Figure 5

(A) Scatter plots denoting the multiple cytokines levels in the serum of mice. (B) Representative flow cytometry analyses denoting the frequencies of Th1 (gated on IFN-γ+CD4+) and Th2 (gated on IL-4+CD4+) cells in CD4+ T cells of anti-CD3 antibody-stimulated splenocytes of MRL/lpr mice (in vitro for 5 h). (C) Scatter plots denoting the Th1 and Th2 cell frequencies in CD4+ T cells of anti-CD3 antibody-stimulated splenocytes of MRL/lpr mice (in vitro for 5 h) and the ratio of Th1/Th2 cells. (D) Representative flow cytometry analyses and scatter plots denoting the frequencies of TNF-producing cells in CD4+ T cells of anti-CD3 antibody-stimulated splenocytes of MRL/lpr mice (in vitro for 5 h). (E) Representative flow cytometry analyses and scatter plots denoting the frequencies of Treg cells (Foxp3+CD25+CD4+) in CD4+ Tcells of mice. Data presented as mean±SD (n=5-9 mice per group) from 2-3 independent experiments: #P < 0.05, ##P < 0.01 by Mann-Whitney U test (comparison of Th2 frequency between Vehicle and CL in Figure 5C) or one-way analysis of variance.

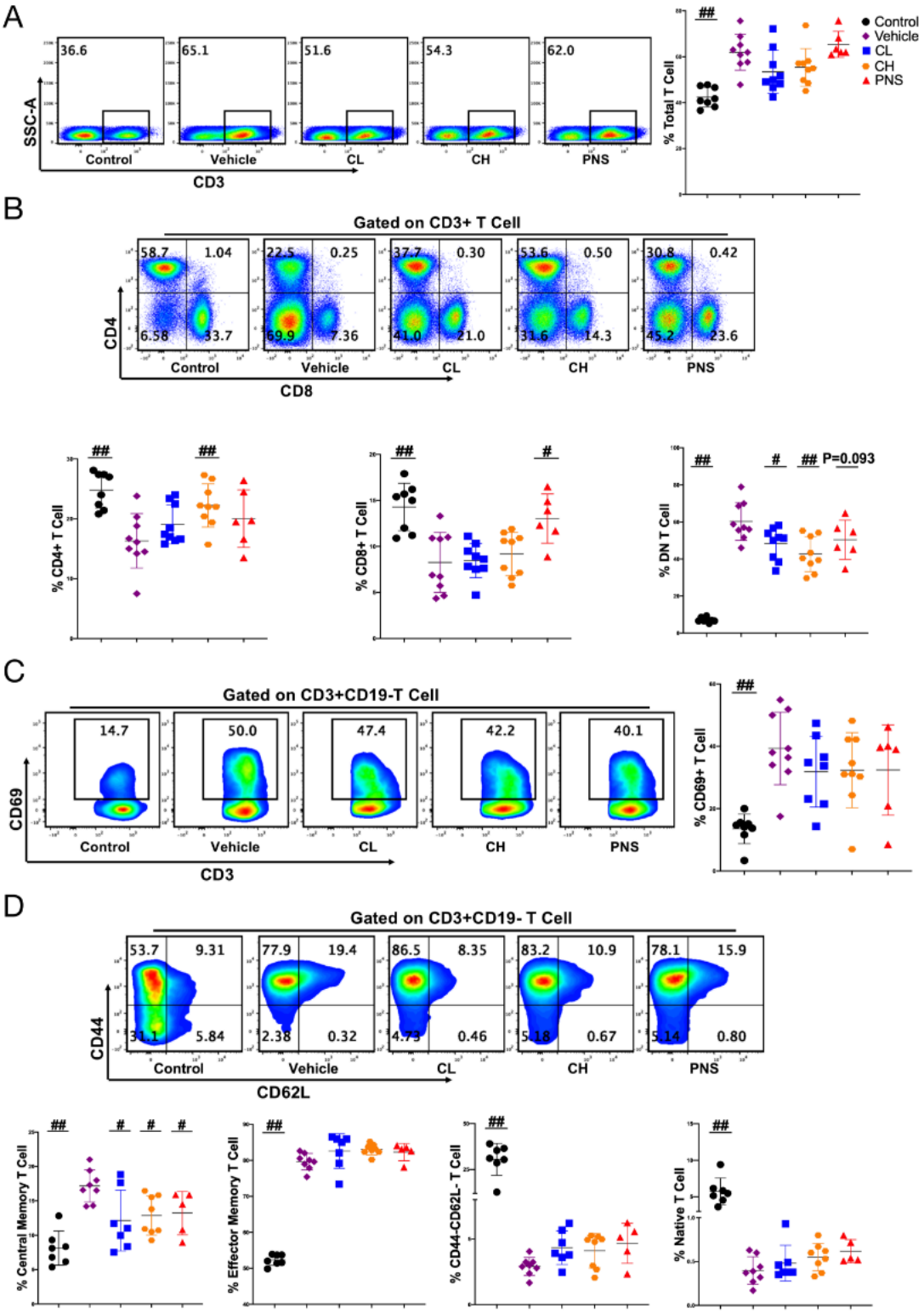


Figure 6

(A) Representative flow cytometry analyses and scatter plots denoting the frequencies of CD3+ total T cells in splenocytes of mice. (B) Representative flow cytometry analyses and scatter plots denoting the frequencies of CD4+ and CD8+ T cells in splenocytes of mice, and frequencies of DN T cells among CD3+ T cells. (C) Representative flow cytometry analyses and scatter plots denoting the frequencies of CD69+ cells in CD3+ T cells of mice. (D) Representative flow cytometry analyses and scatter plots

denoting the frequencies of central memory (CD44+CD62L+), effector memory (CD44+CD62L-), native (CD44-CD62L+), and CD44-CD62L- T cells in CD3+ T cells of mice. Data presented as mean±SD (n=6-9 mice per group) from 2-3 independent experiments: #P < 0.05, ##P < 0.01 by one-way analysis of variance.

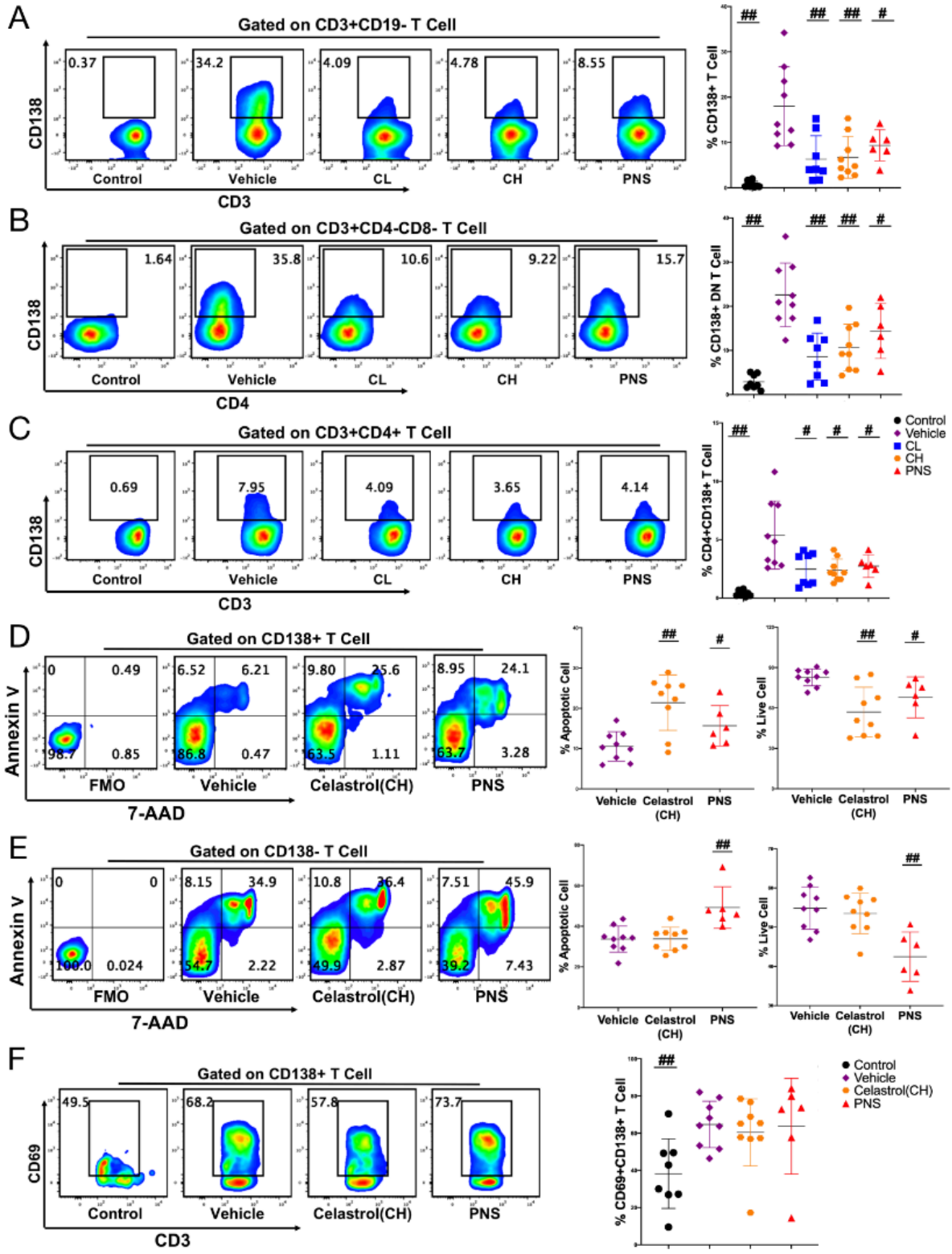


Figure 7

(A) Representative flow cytometry analyses and scatter plots denoting the frequencies of CD138+ cells among CD3+ T cells in mice. (B) Representative flow cytometry analyses and scatter plots denoting the frequencies of CD138+ cells in DN T cells of mice. (C) Representative flow cytometry analyses and scatter plots denoting the frequencies of CD138+ cells in CD4+ T cells of mice. (D) Representative flow cytometry analyses and scatter plots denoting the frequencies of apoptotic and live cells in CD138+ T cells of mice. (E) Representative flow cytometry analyses and scatter plots denoting the frequencies of apoptotic and live cells in CD138- T cells of mice. (F) Representative flow cytometry analyses and scatter plots denoting the frequencies of CD69+ cells in CD138+ T cells of mice. Data presented as mean±SD (n=6-9 mice per group) from 2-3 independent experiments: #P < 0.05, ##P < 0.01 by Kruskal-Wallis H test (Figure 7E) or one-way analysis of variance.